A PRELIMINARY ASSESSMENT OF THE WSR-88D HAIL DETECTION ALGORITHM'S PERFORMANCE OVER NORTHERN OHIO AND NORTHWEST PENNSYLVANIA

Kevin M. Barjenbruch
and
Robert E. LaPlante

NOAA/National Weather Service Forecast Office
Cleveland, Ohio

Abstract

Detecting large hail is an important component of the NOAA/National Weather Service's (NWS) mission of detecting and warning for severe local storms. The NOAA/National Severe Storms Laboratory (NSSL) has developed a new Hail Detection Algorithm (HDA). This HDA was implemented with Weather Surveillance Radar-1988 Doppler (WSR-88D) software Build 9.0 in October of 1996 and replaced the original HDA implemented with the installation of the WSR-88D network. The purpose of this study was to assess the performance of the HDA and to suggest guidance criteria for issuing severe thunderstorm warnings for the Lake Erie region based on the Probability Of Severe Hail (POSH) and Maximum Expected Hail Size (MEHS).

The HDA was evaluated through the use of the WSR-88D Algorithm Testing and Display System (WATADS), which processes, analyzes, and displays WSR-88D Level II data. The HDA output was compared to Storm Data on a scan by scan basis. This scan by scan approach was used to tailor the results of this study to the operational radar meteorologist, who must make a warn/no warn decision for each scan.

An examination of all cases showed that the HDA overforecasts the occurrence of severe hail. A lack of ground truth observations in rural areas contributed to this result. When only counties with high population densities were examined, the HDA overforecasting of severe hail decreased. An analysis of the MEHS estimates indicated that the HDA has skill in determining severe hail size. The results of this study indicated that radar operators should consider issuing a severe thunderstorm warning if the HDA POSH is ≥ 70% and other severe weather signatures are present in the radar data.

1. Introduction

Detecting large hail is an important component of the NOAA/National Weather Service's (NWS) mission of detecting and warning for severe local storms. Hail causes nearly one billion dollars in damage to property and crops annually.

During severe weather operations, NWS forecasters typically review radar data on a scan by scan basis, as one method for determining if a severe thunderstorm warning based on hail potential is necessary. The current United States criteria for identifying a severe thunderstorm require that the thunderstorm produces hail equal to or greater than three quarters of an inch (1.9 centimeters) in diameter and/or winds of 58 miles per hour or greater.

In October of 1996, a new Hail Detection Algorithm (HDA) (Witt 1996) was implemented with Weather Surveillance Radar-1988 Doppler (WSR-88D) Software Build 9.0. This HDA replaced the original HDA implemented with the installation of the WSR-88D network (Klazura and Imy 1993). The improved HDA was developed by the NOAA/National Severe Storms Laboratory (NSSL) and searches for high reflectivities above the freezing level (Witt 1996). This algorithm was designed to work independent of the storm type, tilt, and overhang. Prior to the implementation of WSR-88D Software Build 9.0, the original HDA assumed all hail storms had supercell reflectivity characteristics.

The original HDA produced one of four possible hail indications: Positive, Probable, None, and Insufficient data (Klazura and Imy 1993), for each storm cell identified. The algorithm did not predict hail size. The new HDA produces Probability of Hail (POH) and Probability of Severe Hail (POSH) values from 0% to 100% in 10% increments (Witt 1996). The algorithm also produces Maximum Expected Hail Size (MEHS) estimates.

The POH and POSH are part of the Hail Index product which is displayed in graphical form on the Principal User Processor (PUP) component of the WSR-88D. The POH is represented with a small open or solid green triangle. Whether the triangle is open or solid depends on a threshold set by the PUP operator for a specific percentage of occurrence. The POSH is represented by a large triangle, again with the solid green triangle representing a specific threshold. The MEHS, rounded to the nearest inch, will be displayed in the center of the POSH symbol. An asterisk will be placed in the center of the POSH symbol for hail less than three quarters of an inch in diameter. The POH, POSH, and MEHS are also displayed in tabular form as part of the Hail Index Attribute Table which is contained within the Hail Index product. Additional information on the Hail Index product can be found in the Build 9.0 Precursor Training Handbook (Operations Training Branch 1996).

The purpose of this study was to assess the performance of the new HDA and to suggest guidance criteria for issuing severe thunderstorm warnings for the Lake Erie region based on the POSH and MEHS. The assessment was completed through the use of the WSR-88D Algorithm Testing

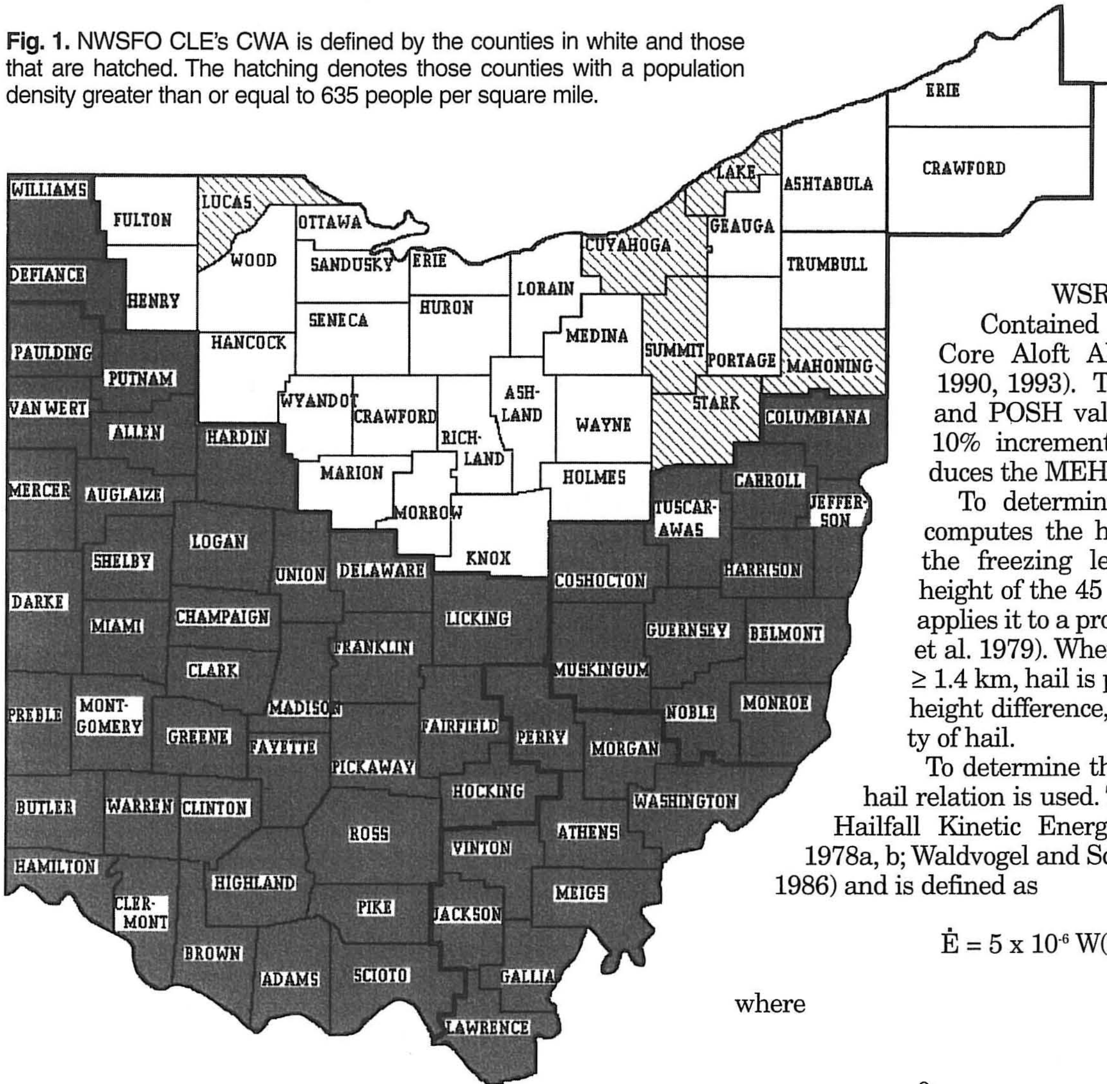

Fig. 1. NWSFO CLE's CWA is defined by the counties in white and those that are hatched. The hatching denotes those counties with a population density greater than or equal to 635 people per square mile.

and Display System (WATADS), developed by the NSSL (McKibben 1996). WATADS processes WSR-88D Level II data through the use of several meteorological algorithms developed by the NSSL.

The data were analyzed for 16 days during which 46 severe hail events occurred within the National Weather Service Forecast Office, Cleveland, Ohio (NWSFO CLE) county warning area (CWA) (Fig. 1). Verification data were taken from *Storm Data* (1995).

Following an assessment of the HDA for all days during which severe hail (hail diameter ≥ 3/4 in.) was recorded, the HDA's performance was evaluated for high population density areas of NWSFO CLE's CWA. The HDA was also evaluated for cases where a sub-storm scale circulation was detected by the WSR-88D Tornado Detection Algorithm (TDA) and/or the Mesocyclone Algorithm (MA) (McKibben 1996). Additionally, the HDA was evaluated for cases when precipitable water (PW) values of the environment were high.

2. Hail Detection Algorithm Description and Input

The HDA runs in conjunction with the WSR-88D Storm Cell Identification and Tracking (SCIT) Algorithm (Witt 1991; Witt and Johnson 1993). The SCIT Algorithm was also developed and tested by the National Severe Storms Laboratory (NSSL) (Witt 1991, 1993), and implemented with WSR-88D software Build 9.0.

Contained in the HDA is the Hail Core Aloft Algorithm (HCAA) (Witt 1990, 1993). The HCAA produces POH and POSH values from 0% to 100% in 10% increments. The HCAA also produces the MEHS estimates.

To determine the POH, the HCAA computes the height difference between the freezing level and the maximum height of the 45 dBZ reflectivity echo and applies it to a probability curve (Waldvogel et al. 1979). When this height difference is ≥ 1.4 km, hail is predicted. The greater the height difference, the higher the probability of hail.

To determine the POSH, a reflectivity to hail relation is used. This relation is called the Hailfall Kinetic Energy ($\dot{E}$) (Waldvogel et al. 1978a, b; Waldvogel and Schmid 1982; Federer et al. 1986) and is defined as

$$\dot{E} = 5 \times 10^{-6}\, W(Z) 10^{0.084Z} \qquad (1)$$

where

$$W(Z) = \begin{cases} 0 & \text{for } Z \leq Z_1 \\ 0.1\,(Z - Z_1) & \text{for } Z_1 < Z < Z_2 \\ 1 & \text{for } Z \geq Z_2 \end{cases}$$

Here, Z is in dBZ, $\dot{E}$ is in J m^{-2} s^{-1}, and Z_1 and Z_2 define a 10 dBZ transition zone. For this algorithm, Z_1 = 40 dBZ and Z_2 = 50 dBZ.

From the above, Hailfall Kinetic Energy is only dependent upon elevated high reflectivity echoes (reflectivity echoes > 40 dBZ above the freezing level) which are associated with hail.

Additionally, the HCAA uses a temperature weighted vertical integration. Since hail growth only occurs above the freezing level, with most of the growth at temperatures ≤ –20°C (English 1973; Browning 1977; Nelson 1983; Miller et al. 1988), the following temperature based weighting function is used

$$WT(H) = \begin{cases} 0 & \text{for } H \leq H_0 \\ \dfrac{H - H_0}{H_{M20} - H_0} & \text{for } H_0 < H < H_{M20} \\ 1 & \text{for } H \geq H_{M20} \end{cases} \qquad (2)$$

where H is the height above ground level (AGL), H_0 is the height AGL of the freezing level, and H_{M20} is the height AGL of the –20 °C environmental temperature.

The resulting parameter is called the Severe Hail Index (SHI) and is defined as

$$SHI = \sum_{i=1}^{N} WT(H_i)\, \dot{E}_i\, \nabla H_i \tag{3}$$

where N is the number of storm components (constant elevation angle slices) for the cell being analyzed, $\dot{E}_i$ is defined in equation (1), and ∇H_i is the height difference (AGL) between elevation angle slices.

The POSH is calculated using the SHI and a warning threshold that is determined from the Warning Threshold Selection Model (WTSM) (Witt 1993). Witt (1993) found that the optimum threshold to warn for severe hail on a given storm day was highly correlated to the melting level, and this relationship was then used to develop the WTSM. A study by Rasmussen and Heymsfield (1987) found that further optimization of the WTSM is possible by including an adjustment based on the average relative humidity below the melting level.

Currently, the WTSM is defined as

$$WT = 57.5(H0) - 121 + A_{RH} \tag{4}$$

where WT is the Warning Threshold, H0 is the melting level, and A_{RH} is the relative humidity adjustment factor, defined as

$$A_{RH} = 160 - 20(DPD_{700}) \tag{5}$$

where DPD_{700} is the 700 mb dew point depression (in °C). In those situations where the DPD_{700} is greater than 8°C or H0 is less than 3.0 km, A_{RH} is set to zero. ***NOTE:*** *A_{RH} has not been incorporated into the current operational WSR-88D HDA. Given the exclusion of A_{RH} in the operational HDA, and since initial study results have indicated that A_{RH} has only a minimal effect on the skill of the HDA (Witt 1996), its value was set to zero for the purpose of this study.*

Witt then developed a relation using observed SHI values and the optimum warning threshold (WT), determined from the WTSM, to calculate representative POSH values. The equation used is

$$POSH = 29 \ln(SHI/WT) + 50 \tag{6}$$

with values < 0 set to 0 and values > 100 set to 100. Since both the WTSM and POSH equations were developed using a fairly small number of hailstorm days, they should be considered experimental and will likely change somewhat as more data is analyzed (Witt 1996).

The SHI is also used to provide estimates of the Maximum Expected Hail Size (MEHS). The equation used is

$$MEHS_{HCAA} = 0.1(SHI)^{0.5} \tag{7}$$

To optimize results from the HDA, WATADS sounder user adjustable parameters were entered for each of the 16 days. Among these were the heights of the 0 °C and –20 °C levels.

3. Methodology

The HDA was evaluated through the use of WATADS which processes, analyzes, and displays WSR-88D Level II data (base reflectivity, base velocity, and spectrum width) (Crum et al. 1993). The POSH and MEHS are displayed by WATADS in tabular form.

The NWSFO CLE (KCLE) WSR-88D archive level II data were processed and analyzed to evaluate the HDA. For approximately 95% of the cases analyzed in this study, Volume Coverage Pattern (VCP) 21, which utilizes nine elevation scans in six minutes, was employed (Crum et al. 1993; Klazura and Imy 1993). VCP 11, which utilizes 14 elevation scans in five minutes, was employed for the remainder of the cases.

Ground truth was obtained solely from *Storm Data*. There were 46 severe hail events during the 16 days examined.

Ground truth reports were checked for spatial and temporal errors using the WATADS display of base reflectivity data. When temporal adjustments were made, the time of the storm report was adjusted based on the radar location of the severe storm and the time of the elevation scan. Temporal adjustments were made for 12 of the events and all adjustments were less than 30 minutes. All ground truth reports with respect to location were valid.

4. Evaluation Procedures

The procedure for relating HDA cell output to severe hail reports was as follows:

a. KCLE WSR-88D archive level II data were processed from 30 min prior to the first report of severe hail until 30 min after the final report of severe hail for each of the 16 days on which severe hail occurred.

b. *Storm Data* hail reports were adjusted temporally to match with storm cells observed in the radar data. No adjustments with respect to location were necessary.

c. Manual scoring was then completed using *Storm Data* and algorithm output files. The scoring was completed as follows:

1) Each cell for which the POSH equaled or exceeded 10% was examined on a scan by scan basis to determine a probability of occurrence of severe hail. This scan by scan approach was used to tailor the results of this study to the operational radar meteorologist, who must make a warn/no warn decision for each scan.

2) *Storm Data* was then examined for each cell for which the POSH was ≥ 10% to determine if that cell could be correlated to an actual severe hail report.

3) Each cell was then scored as a hit or a false alarm.

Only 20 cells can be displayed in the WATADS Cell Table for any given volume scan. The cells are weighted by severity, then listed in order of decreasing severity. Thus, during active severe weather periods, some cells with a low POSH were not listed and consequently, not evaluated.

The data were then stratified three different ways to further access the algorithm's performance.

The TDA contained in WATADS detects the Tornadic Vortex Signature (TVS) circulation pattern. The MA contained in WATADS detects the following circulations: Mesocyclone associated with a TVS (TORMES), Mesocyclone (MESO), Low-topped Mesocyclone (LOWTOP), Couplet (CPLT), Low-altitude Circulation (LOWALT), Long-range Circulation (2DFT), Weak Circulation (WKCIRC), 3D Weak Couplet (WKCPLT), Weak Low-altitude Circulation (WKLALT), and Weak Long-range Circulation (WK2DFT) (McKibben 1996).

Of the above circulations, three were detected by the WATADS algorithms in this study: MESO, WKCIRC, and WKCPLT.

The operational WSR-88D Tornado Vortex Signature (TVS) Algorithm detects a Tornadic Vortex Signature (TVS) circulation pattern, while the Mesocyclone Algorithm detects Mesocyclone (MESO), 3-D Correlated Shear, and Uncorrelated Shear circulation patterns (Klazura and Imy 1993).

Since storm rotation implies dynamic updraft forcing and a high degree of storm organization, severe hail should occur more frequently if a circulation is present.

While the WATADS detected circulations and the operational WSR-88D circulations are defined differently, the presence of any circulation may be an indicator of the presence of severe hail. Thus, the data were stratified by the type of circulation present to look for an enhancement in the HDA's performance.

If the HDA POSH and WSR-88D circulation signatures could be more closely correlated to the actual occurrence of severe hail, then the radar operator could issue severe thunderstorm warnings with a greater degree of confidence that the warnings would verify.

Due to a lack of ground truth in data sparse areas, a separate evaluation of the algorithm's performance was completed for high population density counties within the NWSFO CLE CWA (six counties with a population density ≥ 635 people per square mile) (Fig. 1). These six counties contained all the metropolitan areas with a population > 100,000 within the NWSFO CLE CWA.

Preliminary findings by Witt at the NSSL (1997, personal communication) and Foster, Science Operations Officer (SOO) at NWSFO Fort Worth, Texas (FTW) (1997, personal communication) indicate that the NSSL HDA tends to overwarn in tropical environments. Thus, an evaluation was completed for high precipitable water (PW) events (PW values ≥ 1.5 in.) to assess the HDA's performance in tropical airmasses.

The Mean Absolute Error (MAE) as defined in equation (8) and Mean Error (ME), equation (9), were computed for all cells with a POSH ≥ 50%, that could be correlated with a severe hail report. The 50% POSH threshold was chosen since it represents the mid-point of the probability scale.

$$\mathrm{MAE} = N^{-1} \sum \left| HS_F - HS_O \right| \tag{8}$$

$$\mathrm{ME} = N^{-1} \sum (HS_F - HS_O) \tag{9}$$

Here, HS_F is the forecast hail size and HS_O is the observed hail size. The ME and MAE were also calculated only for the scan prior to each severe hail report if the above conditions were met.

Next, the lead time (time from when the HDA indicated a POSH ≥ 50% to the time of the severe hail) was calculated for each event.

Finally, the Probability of Detection (POD), False Alarm Ratio (FAR), and Critical Success Index (CSI) were calculated based upon a POSH ≥ 50%.

5. Performance Results

Using the evaluation procedure given in Section 4, algorithm performance results were generated for all storm days analyzed. Given that the results below are based on just 16 days from one severe weather season, the sample size should be taken into account when viewing the results of this study. The sample sizes for the 90% and 100% HDA POSH thresholds are especially limited, with just 10 and 15 cases, respectively.

Table 1. Observed probability of severe hail for all convective cells with a HDA POSH ≥ 10%.

HDA POSH (%)	10	20	30	40	50	60	70	80	90	100
Observed severe hail frequency (%)	5	8	13	9	24	30	25	27	50	73
Number of Cells	147	168	171	193	165	100	76	49	10	15

Table 1 contains the observed probability of severe hail for all convective cells with a HDA POSH ≥ 10%. For all days analyzed, the HDA significantly overforecast the occurrence of severe hail. The difference between the POSH and the percentage of time that severe hail occurred ranged from 5% for the 10% POSH threshold to 53% for the 80% threshold. An apparent contributor to the poor performance of the algorithm was the lack of ground truth reports in rural areas.

The HDA was evaluated for the six counties of NWSFO CLE's CWA with the greatest population density (Fig. 1) in an attempt to determine the algorithm's performance in areas where ground truth reports are more easily obtainable. The six counties were: Cuyahoga, Lake, Lucas, Mahoning, Stark, and Summit; all are in Ohio and each has a population density ≥635 people per square mile.

Table 2. Observed probability of severe hail for cells in urban areas with a HDA POSH ≥ 10%.

HDA POSH (%)	10	20	30	40	50	60	70	80	90	100
Observed severe hail frequency (%)	13	15	14	27	37	32	53	60	100	–
Number of Cells	32	34	29	30	35	19	15	5	1	0

An analysis of the HDA performance for this data set (Table 2 and Fig. 2) indicated a large improvement, although the trend was still to overforecast severe hail. The exceptions were the 10% POSH threshold, where the observed severe hail frequency was 13%, and the 90% POSH threshold, where the observed severe hail frequency was 100%, though just one cell was included in this

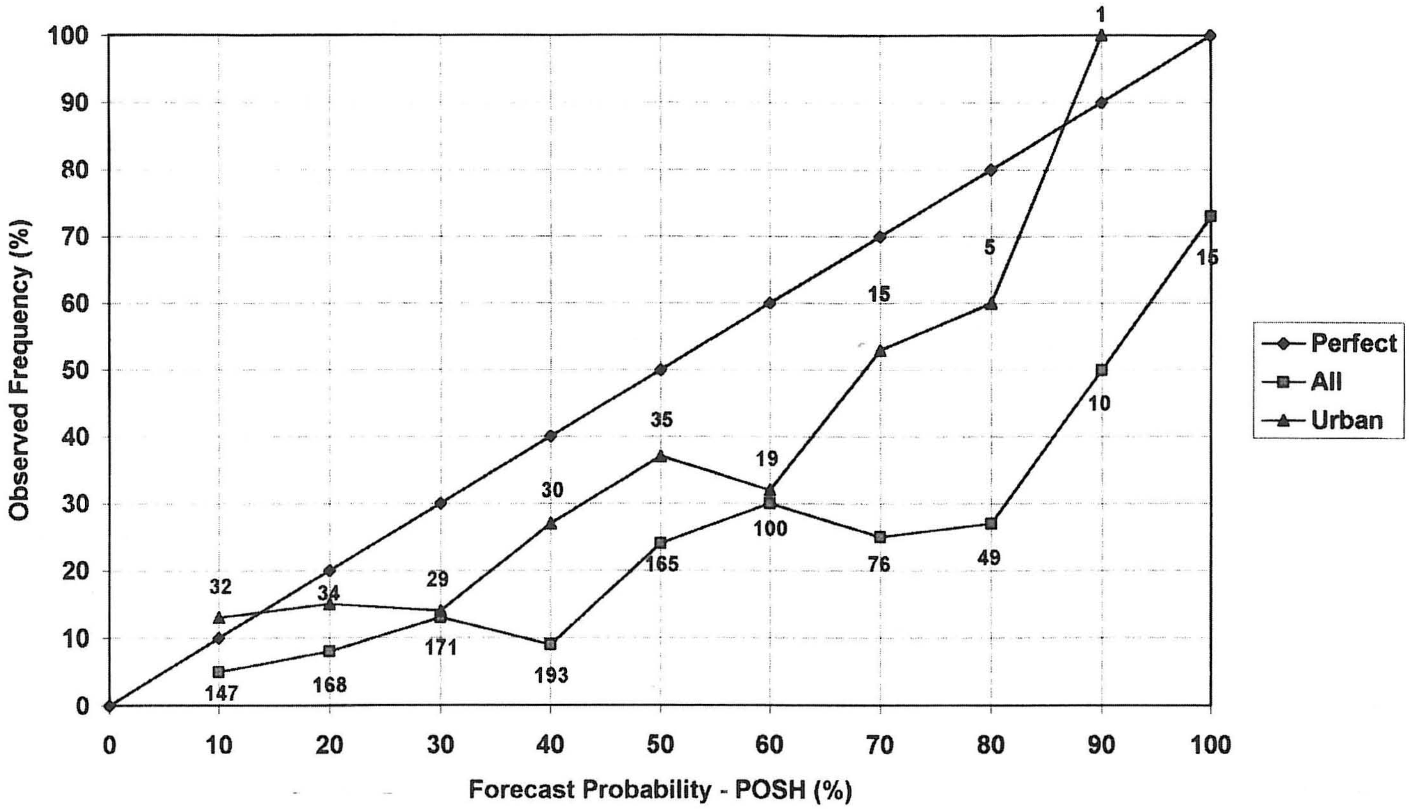

Fig. 2. Observed frequency of severe hail for all cells and for urban cells, with a HDA POSH ≥ 10%. The number of cells for each POSH threshold is plotted for each curve.

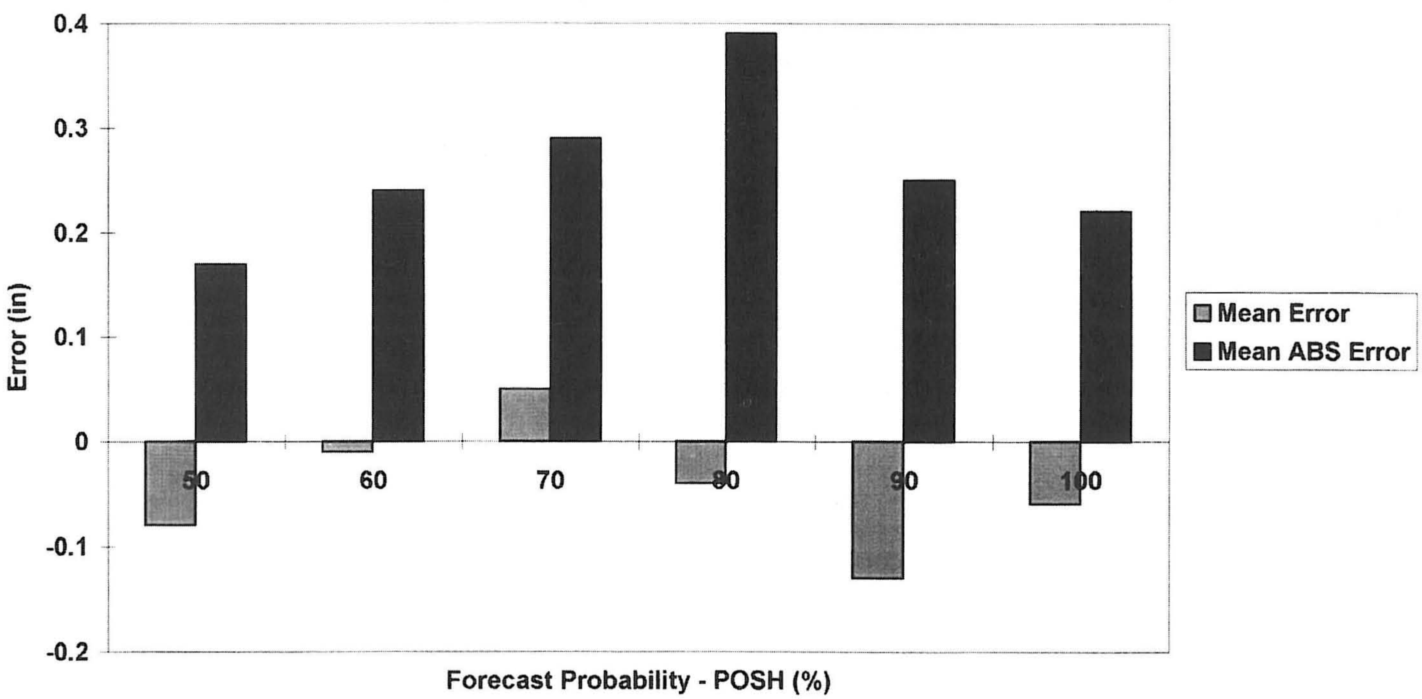

Fig. 3. MAE and ME of MEHS for all cells with a HDA POSH ≥ 50%.

threshold. For the other thresholds, the difference between the POSH and the percentage of time that severe hail occurred ranged from just 5% at the 20% POSH threshold to 28% at the 60% threshold. For a POSH of 70%, severe hail occurred 53% percent of the time. For the 80% threshold, severe hail occurred 60% of the time. Since the observed severe sized hail frequency is > 50% when the POSH is ≥ 70%, radar operators should consider issuing a severe thunderstorm warning if the HDA POSH is ≥ 70% and other severe weather signatures are present in the radar data.

Table 3. Observed probability of severe hail for cells with a MESO circulation pattern and a HDA POSH ≥ 10%.

HDA POSH (%)	10	20	30	40	50	60	70	80	90	100
Observed severe hail frequency (%)	–	–	–	–	–	–	–	–	–	100
Number of Cells	0	0	0	0	0	0	0	0	0	1

Table 4. Observed probability of severe hail for cells with a WKCIRC circulation pattern and a HDA POSH ≥ 10%.

HDA POSH (%)	10	20	30	40	50	60	70	80	90	100
Observed severe hail frequency (%)	50	13	11	17	16	44	0	43	0	75
Number of Cells	2	15	9	12	19	9	11	7	1	8

Table 5. Observed probability of severe hail for cells with a WKCPLT circulation pattern and a HDA POSH ≥ 10%.

HDA POSH (%)	10	20	30	40	50	60	70	80	90	100
Observed severe hail frequency (%)	0	0	29	8	21	27	17	25	–	100
Number of Cells	7	8	7	12	14	11	12	8	0	1

Data were then stratified by the presence of three circulation patterns to determine if the presence of these signatures could be correlated to the performance of the HDA. The three circulation patterns were Mesocyclone (MESO), Weak Circulation (WKCIRC), and Weak Couplet (WKCPLT). These circulation patterns are detected by The Mesocyclone Detection Algorithm. For this study, a circulation was detected in 174 cells. A MESO was detected in only one cell, a WKCIRC was detected in 93 cells, and a WKCPLT was detected in 80 cells. Classification by circulation present (Tables 3–5), indicated no improvement in the HDA performance.

To evaluate the HDA for different airmasses, the HDA performance was examined for each day that the PW value of the environment was ≥ 1.5 in. A comparison of the high PW subset and the entire sample (Tables 1 and 6), indicated similar HDA results. Severe hail could not be correlated with any cells with a POSH of 90% or 100%, though the sample size was limited to just 4 and 3 events, respectively. Thus, classification by the PW value indicated essentially no change in the performance of the HDA.

Table 6. Observed probability of severe hail for cells which occurred when the PW value was ≥ 1.5 in. and a HDA POSH ≥ 10%.

HDA POSH (%)	10	20	30	40	50	60	70	80	90	100
Observed severe hail frequency (%)	6	8	17	9	25	36	31	22	0	0
Number of Cells	78	93	102	107	99	76	48	32	4	3

Table 7. MAE and ME of MEHS for all cells with a HDA POSH ≥ 50%.

HDA POSH (%)	50	60	70	80	90	100
MAE of MEHS (in.)	0.17	0.24	0.29	0.39	0.25	0.22
ME of MEHS (in.)	-0.08	-0.01	0.05	-0.04	-0.13	-0.06
Number of Cells	39	32	19	14	4	9

For the HDA POSH thresholds ≥ 50%, the MAE and ME (Table 7 and Fig. 3) were calculated for the MEHS. The MAE was approximately 0.25 in. for all cases combined. The MAE was greatest, 0.39 in., for the 80% POSH threshold and smallest, 0.17 in., for the 50% POSH threshold. An analysis of the ME indicates a tendency to underforecast hail size, though the error was less than 0.10 in. for all but one threshold (POSH of 90%).

The MAE and ME were also computed for the radar scan prior to each event. The errors indicated similar results to the above.

A POSH of ≥ 50% was used to specify if a cell had severe hail for verification purposes. Of the 46 severe hail events included in this study, 37 were detected by the HDA, with nine being missed. This produced a Probability of Detection (POD) score of 0.80. Of the 154 cells with a POSH ≥ 50%, 117 could not be correlated to a ground truth report of severe hail, yielding a False Alarm Ratio (FAR) of 0.76. The resultant Critical Success Index (CSI) was 0.23.

Two of the nine missed events were attributable to the storm cell being within the "cone of silence" of the KCLE radar. No definite conclusions could be reached for the remaining seven missed events.

The POD, FAR, and CSI were also calculated based upon a POSH of ≥ 70%, given the recommended issuance of a severe thunderstorm warning if the POSH equals or exceeds 70%. This produced a POD of 0.52 and a FAR of 0.69. The resultant CSI was 0.24. Compared to the ≥ 50% sample, the POD was reduced, but the FAR decreased. The resultant CSI showed only a minimal improvement.

The POD, FAR, and CSI were also calculated using a POSH of ≥ 70% for the six counties of NWSFO CLE's CWA with the greatest population density. For this subset, the POD was 0.36, the FAR was 0.58, and the resultant CSI was 0.24. It should be noted that the sample size of this subset was rather small.

Using a POSH of ≥ 50% to determine if a cell had severe hail, the average lead time of the HDA for the occurrence of severe hail was 19 minutes.

Based on a POSH of ≥ 70%, the average lead time was 13 minutes. Based on a POSH of ≥ 70% for the high population density counties, the average lead time was 16 minutes.

6. Conclusions

A limited study of the performance of the operational HDA has been conducted over northern Ohio using KCLE WSR-88D data for 16 convective days in 1995. Obtaining complete and accurate ground truth verification data are critical in determining the HDA algorithm's true performance.

An examination of all cases showed that the algorithm overforecasts the occurrence of severe hail. However, a lack of ground truth observations in rural areas likely contributed to this result. When only counties with a population density ≥ 635 people per square mile were examined, the HDA's overforecasting of severe hail decreased. The sample size in this study was small and the results presented here are preliminary, especially for the threshold categories of 90% and 100%, which were only comprised of a few cases. The results indicated that radar operators should consider issuing a severe thunderstorm warning if the HDA POSH is ≥ 70% and other severe weather signatures are present in the radar data.

When cases were stratified for the presence of circulation patterns or the amount of precipitable water, little change in the HDA performance was noted.

An analysis of the MEHS estimates, indicated HDA skill in determining severe hail size, with a MAE near 0.25 in. There was a tendency for the size of the severe hail to be underpredicted, though the error was only around 0.10 in.

The HDA did not produce a POSH ≥ 50% for nine of the 46 severe hail reports. Based upon a POSH ≥ 70%, 22 of the 46 severe hail reports were not detected.

With a CSI of 0.23 and a POSH ≥ 50%, it is apparent that the HDA should only be used for guidance. Nothing can replace a comprehensive evaluation of individual storms by the radar operator and a knowledge of the environment the storms are forming in. Although the algorithm appears to be an improvement to the previous algorithm, it still performs inadequately and radar operators need to be cautious when using it.

Acknowledgments

The authors would like to thank James Campbell, the Data Acquisition Program Manager at the NEXRAD Weather Service Forecast Office in Charleston, West Virginia for providing the atmospheric sounding data for Wilmington, Ohio and Pittsburgh, Pennsylvania. The authors also thank the staff of the NOAA/National Climatic Data Center for providing WSR-88D Level II data. Additionally, we appreciate the thorough and insightful review of this manuscript by Gary Carter, Chief, Scientific Services Division, and Laurie Hermes of the Observations and Facilities Branch, both of the National Weather Service Eastern Region Headquarters. Finally, thanks are in order to Brad Vrcek, for his assistance with the figures and to Donald Miller, for his assistance in the processing of the WSR-88D Level II data.

Authors

Robert E. LaPlante is the Science and Operations Officer (SOO) at the National Weather Service Office (NWSO) in Cleveland, Ohio. He received his B.S. degree in Physical Sciences from the University of Maryland in 1983 and his M.S. degree in Meteorology from the University of Maryland in 1986. He joined the NWS in 1986 and worked in the Office of Meteorology at Weather Service Headquarters. In 1988, he transferred to Charleston, West Virginia as a journeyman forecaster. In 1992, he transferred to Topeka, Kansas as a lead forecaster. In 1994, he transferred to Cleveland, Ohio as the SOO.

Kevin Barjenbruch is a General Forecaster at the NWSO in Cleveland, Ohio. He received his B.S. degree in Meteorology from the University of Nebraska at Lincoln in 1987. Prior to accepting a forecaster position at the Cleveland office in 1992, he was a Meteorologist in Training at the NWS office in Fort Wayne, Indiana.

References

Browning, K. A., 1977: The structure and mechanisms of hailstorms. *Hail: A Review of Hail Science and Hail Suppression. Meteor. Monogr.*, No. 38, G. B. Foote and C. A. Knight, Eds., Amer. Meteor. Soc., 1-43.

Crum, T. D., R. L. Alberty, and D. W. Burgess, 1993: Recording, archiving, and using WSR-88D data. *Bull. Amer. Meteor. Soc.*, 74, 645-653.

English, M., 1973: *Alberta Hailstorms*. Part II: Growth of large hail in the storm. *Meteor. Monogr.*, No. 36, Amer. Meteor. Soc., 37-98.

Federer, B., A. Waldvogel, W. Schmid, H. H. Schiesser, F. Hampel, M. Schweingruber, W. Stahel, J. Bader, J. F. Mezeix, N. Doras, G. D'Aubigny, G. DerMegreditchian, and D. Vento, 1986: Main results of Grossversuch IV. J. *Climate Appl. Meteor.*, 25, 917-957.

Klazura, G. E. and D. A. Imy, 1993: A description of the initial set of analysis products available from the NEXRAD WSR-88D system. *Bull. Amer. Meteor. Soc.,* 74, 1293-1311.

McKibben, L., 1996: *WSR-88D Algorithm Testing and Display System*. Stormscale Research and Applications Division.

Miller, L. J., J. D. Tuttle, and C. A. Knight, 1988: Airflow and hail growth in a severe northern High Plains supercell. *J. Atmos. Sci.*, 45, 736-762.

Nelson, S. P., 1983: The influence of storm flow structure on hail growth. *J. Atmos. Sci.*, 40, 1965-1983.

NOAA, 1996: Build 9.0 Precursor Training, 9-12, Operations Training Branch.

NOAA, 1995: *Storm data and unusual weather phenomena with late reports and corrections*, 37(4-11), NESDIS, National Climatic Data Center.

Rasmussen, R. M., and A. J. Heymsfield, 1987: Melting and shedding of graupel and hail. Part II: Sensitivity study. *J. Atmos. Sci.* 19, 2764-2782.

Waldvogel, A., W. Schmid, and B. Federer, 1978a: The kinetic energy of hailfalls. Part I: Hailstone spectra. *J. Appl. Meteor.*, 17, 515-520.

________, B. Federer, W. Schmid, and J. F. Mezeix, 1978b: The kinetic energy of hailfalls. Part II: Radar and hailpads. *J. Appl. Meteor.*, 17,1680-1693.

________, B. Federer and P. Grimm, 1979: Criteria for the detection of hail cells. *J. Appl. Meteor.*, 18, 1521-1525.

________, and W. Schmid, 1982: The kinetic energy of hailfalls. Part III: Sampling errors inferred from radar data. *J. Appl. Meteor.*, 21, 1228-1238.

Witt, A., 1990: A hail core aloft detection algorithm. Preprints: *16th Conf. on Severe Local Storms*, Alberta, Amer. Meteor. Soc., 232-235.

________, 1991: The new NSSL storm cell tracking algorithm. Report for the WSR-88D OSF, 10pp.

________, 1993: Comparison of the performance of two hail detection algorithms using WSR-88D data. Preprints: *26th Intl. Conf. on Radar Meteorology*, Norman, Amer. Meteor. Soc., 154-156.

________, and J. T. Johnson, 1993: An enhanced storm cell identification and tracking algorithm. Preprints: *26th Intl. Conf. on Radar Meteorology*, Norman, Amer. Meteor. Soc., 141-143.

________, 1996: *The NSSL Hail Detection Algorithm.* The WSR-88D Operational Support Facility, 40pp.